JOC Article
pubs.acs.org/joc

Solid-State Molecular Rotors with Perdeuterated Stators: Mechanistic Insights from Biphenylene Rotational Dynamics in Ordered and Disordered Crystal Forms

Zachary J. O'Brien, Steven D. Karlen, Saeed Khan, and Miguel A. Garcia-Garibay*

Department of Chemistry and Biochemistry, University of California, Los Angeles, California 90095-1569

mgg@chem.ucla.edu

Received November 26, 2009

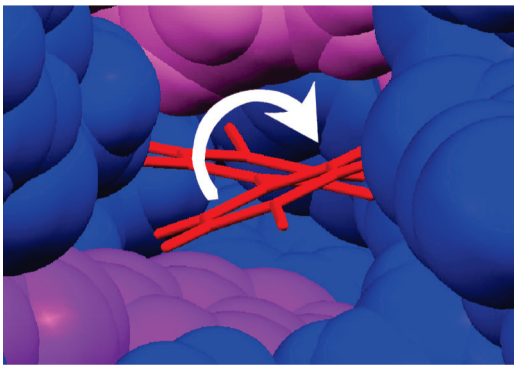

Samples of 4,4′-bis(3,3,3-tri-d_5-phenylpropynyl)biphenyl **2**, 9,10-bis(3,3,3-tri-d_5-phenylpropynyl)-anthracene **3**, 1,4-bis(3,3,3-tri-d_5-phenylpropynyl)naphthalene **4**, and 4,4′-bis(3,3,3-tri-d_5-phenyl-propynyl)-1,1′-binaphthyl **5** were prepared via a Sonogashira coupling of 3,3,3-tri-d_5-phenylpropyne **7** and the appropriate aryl dibromide. Single crystal X-ray diffraction structures were obtained for an *o*-xylene clathrate of **2** and for solvent-free crystals of **3**. All four molecular rotors were characterized by CPMAS ^{13}C NMR experiments with varying contact times in order to determine whether the carbon signals of the central rotator group could be selectively enhanced and studied without interference or overlap of signals from the deuterated stator, which is insensitive to the $\{^1H\}$-^{13}C cross-polarization method. It was shown that the ^{13}C signals of the natural abundance rotator group can be selectively observed with short contact times (ca. 50 μs) without interference from other ^{13}C signals in the molecule. Variable-temperature CPMAS ^{13}C NMR studies with a crystalline *o*-xylene solvate of biphenylene rotor **2** suggested a 2-fold flipping process in the fast exchange regime, even at temperatures as low as 199 K (−74 °C). Indirect support for this was obtained by studies carried out with a disordered, solvent-free solid, obtained by fast precipitation from hexanes and dichloro-methane, which displayed slower dynamics within the same temperature range with an activation energy of 8.7 kcal/mol and a pre-exponential factor of 4.9×10^9 s^{-1}. Confirmation of an exchange process in the megahertz regime for the crystalline solvate was obtained by variable-temperature quadrupolar echo ^{2}H NMR data acquired with samples prepared with a deuterated biphenylene rotator and a natural abundance stator. Although rotational exchange occurs in the solvated samples with a slightly lower barrier of 7.4 kcal/mol, the main difference with the precipitated solid comes from the pre-exponential factor, which is nearly 3 orders of magnitude greater with a value of 2.5×10^{12} s^{-1}. On the basis of these differences, we speculate that efficient rotational motion in the solvated crystals may take advantage of long-range lattice vibrations that couple with molecular modes and that the lack of long-range order may be responsible for the low pre-exponential factor observed in the disordered crystals.

 Published on Web 03/16/2010 DOI: 10.1021/jo9025176

Introduction

Among the new venues of artificial molecular machinery,[1] studies have centered recently on the potential of molecular,[2] coordination,[3] and extended solids,[4] built with structures that form a static lattice linked to elements that experience rapid conformational motions.[5] With components at the two ends of the dynamic spectrum, we proposed the term "amphidynamic solids" to describe the contrasting properties of these materials.[2] Studies in our group have been primarily centered on molecular rotors[6] based on 1,4-bis-(triarylpropynyl)benzene[7] and related structures[2,8] with the expectation that the two axially disposed and relatively bulky triarylpropynyl groups acting as a stator[6] will provide a low density "pocket", where the central phenylene moiety can play the role of the rotator.[6] With structural similarities to macroscopic gyroscopes, these molecular rotors exhibit Brownian rotation in the solid state with ambient temperature exchange frequencies that range from static to ca. 10^9 s^{-1}.[2,7,8] While the long-term goal of these studies is to help advance the fields of functional materials and molecular machinery,[9] short-term goals include investigations of the types of structural features and supramolecular architectures that facilitate fast motion in the solid state and the development of analytical tools to aid the study of such phenomena.

One of the most powerful techniques for the study and characterization of internal motions in the solid state is ^{13}C NMR obtained under cross-polarization and magic angle spinning (CPMAS).[10] The technique allows the acquisition of high-resolution spectra with polycrystalline powder samples, which under favorable circumstances can be used to characterize the molecular motions reported by nuclei experiencing dynamic exchange between magnetically nonequivalent sites.[11] The CPMAS experiment has three key components that improve the sensitivity and resolution of the spectrum. The cross-polarization (CP) part is responsible for signal enhancement by transferring the magnetization from the abundant and sensitive ^1H nuclei to the far less abundant and insensitive ^{13}C nuclei. Rapid sample spinning (e.g., 10 kHz) at the "magic" angle (54.74° relative to the external magnetic field) removes the line-broadening that arises from chemical shift anisotropy. The third component is a strong broadband decoupling RF field that helps remove the dipolar interactions between the ^{13}C and ^1H nuclei.

The intensity of the ^{13}C signals in the CPMAS experiment is a time-dependent function of cross-polarization and depends on the strength of the $^1H-^{13}C$ dipolar coupling. The intensity of a given signal will depend on the number and distance of nearby hydrogen atoms and on the "contact time" allowed for cross-polarization. In a previous communication we showed that the dependence of signal intensity to the presence of nearby hydrogen atoms may be used to highlight signals of interest among many interfering ones by selectively substituting the latter with ^2H nuclei.[12] Using samples of 1,4-bis(3,3,3-tri-d_5-phenylpropynyl)benzene **1** with a perdeuterated bis(trityl)-stator and a natural abundance 1,4-phenylene rotator, we were able to carry out a detailed variable-temperature (VT) analysis of the exchange dynamics of the central phenylene in desolvated crystals of **1**. In this article, we explore the generality of the method with a set of structures that includes 4,4′-biphenylene (**2**), 9,10-anthrylidene (**3**), 1,4-naphthylidene (**4**), and 4,4′-(1,1-binaphthylidene) (**5**) playing the roles of potential rotators (Figure 1). While the bulk of the central aromatics in compounds **3**−**5** and the modest shielding of unsubstituted trityl groups suggest that rotation in the solid state is unlikely, we selected them as valuable test systems because they have well-characterized chromophores that we plan to use in the future with a set of bulkier, more shielding stators. We expected and confirmed that the biphenyl rotator of **2** experiences relatively fast rotational dynamics in the solid state. After showing that the rate of exchange in the case of **2** is too large to be measured with confidence within the temperature limits of our spectrometer by CPMAS ^{13}C NMR ($T \geq 200$ K), we carried out its dynamic characterization by quadrupolar

(1) (a) Michl, Josef; Sykes, E.; Charles, H. *ACS Nano* **2009**, *3*, 1042–1048. (b) Garcia-Garibay, M. A. *Nat. Mater.* **2008**, *7*, 431–432. (c) Garcia-Garibay, M. A. *Angew Chem., Int. Ed.* **2007**, *46*, 8945–8947.

(2) (a) Garcia-Garibay, M. A. *Proc. Natl. Acad. of Sci. U.S.A.* **2005**, *102*, 10793. (b) Khuong, T.-A.; Nuñez, J.; Godinez, C.; Garcia-Garibay, M. *Acc. Chem. Res.* **2006**, *39*, 413–422. (c) Karlen, S. D.; Garcia-Garibay, M. A. *Top. Curr. Chem.* **2006**, *262*, 179–228. (d) Harada, J.; Ogawa, K. *Chem. Soc. Rev.* **2009**, *38*, 2244–2252. (e) Nakai, H.; Nonaka, T.; Miyano, Y.; Mizuno, M.; Ozawa, Y.; Toriumi, K.; Koga, N.; Nishioka, T.; Irie, M.; Isobe, K. *J. Am. Chem. Soc.* **2008**, *130*, 17836–17845.

(3) (a) Akutagawa, T.; Shitagami, K.; Nishihara, S.; Takeda, S.; HasegawaT.; Nakamura, T.; Hosokoshi, Y.; Inoue, K.; Ikeuchi, S.; Miyazaki, Y.; Saito, K. *J. Am. Chem. Soc.* **2005**, *127*, 4397–4402. (b) Akutagawa, T.; Endo, D.; Kudo, F.; Noro, S.-I.; Takeda, S.; Cronin, L.; Nakamura, T. *Crys. Growth Des.* **2008**, *8*, 812–816. (c) Akutagawa, T.; Sato, D.; Koshinaka, H.; Aonuma, M.; Noro, S.-I.; Takeda, S.; Nakamura, T. *Inorg. Chem.* **2008**, *47*, 5951–5962. (d) Akutagawa, T.; Nakamura, T. *Dalton Trans.* **2008**, *45*, 6335–6345. (e) Kitagawa, H.; Kobori, Y.; Yamanaka, M.; Yoza, K.; Kobayashi, K. *Proc. Nat. Acad. Sci. U.S.A.* **2009**, *106*, 10444–10448.

(4) (a) Gould, S. L.; Tranchemontagne, D.; Yaghi, O. M.; Garcia-Garibay, M. A. *J. Am. Chem. Soc.* **2008**, *130*, 3246–3247. (b) Winston, E. B.; Lowell, P. J.; Vacek, J.; Chocholousova, J.; Michl, J.; Price, J. C. *Phys. Chem. Chem. Phys.* **2008**, *10*, 5188–5191. (c) Bracco, S.; Comotti, A.; Valsesia, P.; Chmelka, B. F.; Sozzani, P. *Chem. Commun.* **2008**, *39*, 4798–4800. (d) Loeb, S. *J. Chem. Soc. Rev.* **2007**, *36*, 226–235. (e) Loeb, S. J. In *Organic Nanostructures*; Atwood, J. L., Steed, J. W., Eds.; Wiley-VCH: Weinheim, 2008; pp 33−61.

(5) Alternatives based on crystalline materials that take advantage of phase transitions have also been suggested: Sokolov, A. N.; Swenson, D. C.; MacGillivray, L. R. *Proc. Nat. Acad. Sci. U.S.A.* **2008**, *105*, 1794–1797.

(6) We have adopted here the terminology suggested by Kottas *et al.* While the term "molecular rotor" is used to describe the entire molecular assembly, the term "rotator" refers to the component whose rotational motion is being considered, and the term "stator" to the component that provides a frame of reference to the describe the motion of the former: Kottas, G. S.; Clarke, L. I.; Horinek, D.; Michl, J. *Chem. Rev.* **2005**, *105*, 1281–1376.

(7) (a) Dominguez, Z.; Dang, H.; Strouse, M. J.; Garcia-Garibay, M. A. *J. Am. Chem. Soc.* **2002**, *124*, 2398–2399. (b) Dominguez, Z.; Dang, H.; Strouse, J. M.; Garcia-Garibay, M. A. *J. Am. Chem. Soc.* **2002**, *124*, 7719–7727. (c) Dominguez, Z.; Khuong, T. A. V.; Sanrame, C. N.; Dang, H.; Nuñez, J. E.; Garcia-Garibay, M. A. *J. Am. Chem. Soc.* **2003**, *125*, 8827–8837. (d) Khuong, T. A. V.; Zepeda, G.; Ruiz, R.; Kahn, S. I.; Garcia-Garibay, M. A. *Cryst. Growth Des.* **2004**, *4*, 15–18. (e) Karlen, S. D.; Ortiz, R.; Chapman, O. L.; Garcia-Garibay, M. A. *J. Am. Chem. Soc.* **2005**, *127*, 6554–6555. (f) Nuñez, J. E.; Khuong, T.-A. V.; Campos, L. M.; Farfan, N.; Dang, H.; Karlen, S. D.; Garcia-Garibay, M. A. *Cryst. Growth Des.* **2006**, *6*, 866–873.

(8) (a) Godinez, C. E.; Zepeda, G.; Garcia-Garibay, M. A. *J. Am. Chem. Soc.* **2002**, *124*, 4701–4707. (b) Godinez, C. E.; Garcia-Garibay, M. A. *Cryst. Growth Des.* **2009**, *9*, 3124–3128.

(9) (a) Leigh, D. A.; Zerbetto, F.; Kay, E. R. *Angew. Chem., Int. Ed.* **2007**, *46*, 72–191. (b) Saha, S.; Stoddart, J. F. *Chem. Soc. Rev.* **2007**, *36*, 77–92. (c) Balzani, V.; Credi, A.; Venturi, M. *Chem. Phys. Chem.* **2008**, *9*, 202–220. (d) Vicario, J.; Katsonis, N.; Ramon, B. S.; Bastiaansen, C. W. M.; Broer, D. J.; Feringa, B. L. *Nature* **2006**, *440*, 163.

(10) Pines, A.; Gibby, M. G.; Waugh, J. S. *J. Chem. Phys.* **1973**, *59*, 569–590.

(11) (a) Braga, D.; Chierotti, M. R.; Garino, N.; Gobetto, R.; Grepioni, F.; Polito, M.; Viale, A. *Organometallics* **2007**, *26*, 2266–2271.

(12) Karlen, S. D.; Garcia-Garibay, M. A. *Chem. Commun.* **2005**, 189–191.

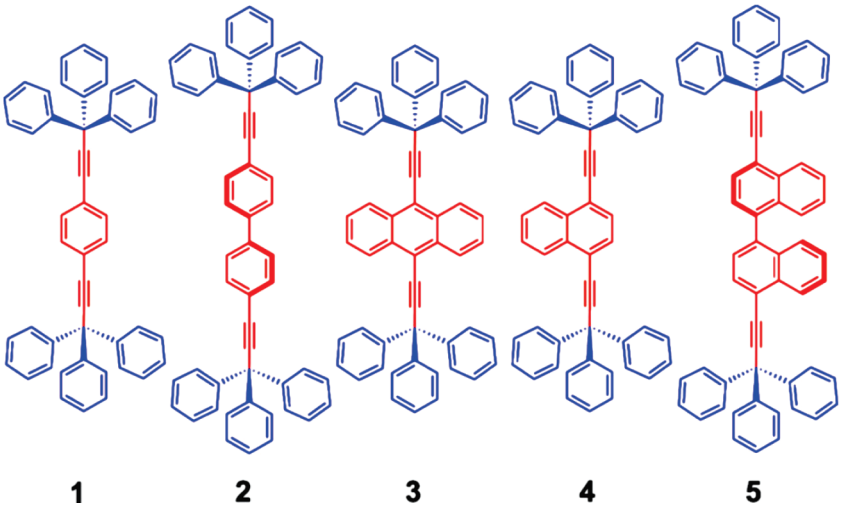

FIGURE 1. Compounds studied using selective cross-polarization to highlight the signals of the rotator.

echo ^{2}H NMR with samples containing a deuterated rotator and a natural abundance stator. While the CPMAS ^{13}C NMR spectral information obtained with compound **3** suggested that there may be sufficient chemical shift dispersion to investigate its rotational dynamics in molecular rotors with larger stators, the spectral resolution observed with compounds **4** and **5** is significantly lower, indicating that a determination of their rotational dynamics by this method should be more challenging.

Results and Discussion

Synthesis and Characterization. Like samples of 1,4-bis(3,3,3-tri-d_5-phenylpropynyl)benzene **1** before,[12] samples of 4,4′-bis(3,3,3-tri-d_5-phenylpropynyl)biphenyl **2**, 9,10-bis(3,3,3-tri-d_5-phenylpropynyl)anthracene **3**, 1,4-bis(3,3,3-tri-d_5-phenylpropynyl)naphthalene **4**, and 4,4′-bis(3,3,3-tri-d_5-phenylpropynyl)-1,1′-binaphthyl **5** were obtained by a straightforward 3-step synthesis from d_6-benzene as illustrated in Scheme 1.

The preparation of d_{15}-3,3,3-triphenylpropyne **7** via Friedel–Crafts alkylation of d_6-benzene with carbon tetrachloride[13] followed by substitution of the resulting chloride by ethynylmagnesium bromide was accomplished in 35.0% overall yield. The final step in the syntheses of compounds **1**–**5** was accomplished via Sonogashira coupling of **7** and the appropriate aryl dibromide in ca. 60% yield after column chromatography (hexanes/C_6H_6/CH_2Cl_2 = 90:5:5). The structures of **1**–**5** were determined by ^{13}C and ^{1}H NMR, attenuated total reflectance (ATR) FTIR, and high-resolution MALDI-TOF mass spectrometry data.

Compounds **1**–**5** all display the characteristic C–D stretch at 2274 cm^{-1} in the IR spectrum as well as the sp^2 C–H stretches at ~3000 cm^{-1}, indicating the presence of both hydrogen and deuterium atoms. Signals that are common to all four samples have a good correspondence in the ^{13}C NMR solution spectra. These include the quaternary trityl carbon at ca. 56 ppm, the two alkyne signals at ca. 96 and 85 ppm, and the signal of the three dynamically averaged ipso-carbons in the trityl groups at ca. 145 ppm. Signals

SCHEME 1

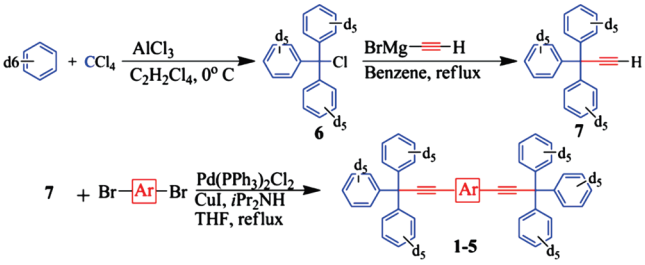

corresponding to the deuterated carbons occur as small triplets in the range of 126–129 ppm. Corresponding weak signals in the ^{1}H NMR spectra occur at ca. 7.4 and 7.3 ppm due to the residual ca. 0.5% of hydrogens present in the starting material.

The characterization and X-ray structure of **1** has been discussed in the detail in the literature.[7a,b,12] The ^{1}H NMR spectrum of **2** is characteristic of symmetric 4,4′-disubstituted 1,1′-biphenyls with a pair of doublets between 7.5 and 7.6 ppm (J = 8.5 Hz) in a 1:1 ratio. Signals at 132.1 and 126.8 ppm in the ^{13}C NMR spectrum correspond to the protonated carbon signals of the biphenyl (C3 and C2, respectively), while peaks at 140.0 and 122.9 ppm correspond to the quaternary aromatic carbon atoms (C1 and C4) of the same moiety.

The NMR spectra of compound **3** are also characteristic of symmetric 9,10-disubstituted anthracenes. The ^{1}H NMR spectrum consists of two complex multiplets of the AA′XX′ system (J_{ax} = $J_{a'x'}$ = 9.0 Hz, $J_{xx'}$ = 8.0 Hz, $J_{aa'}$ = 0.8 Hz, $J_{ax'}$ = $J_{a'x}$ = 2.1 Hz) at 8.57 and 7.53 ppm, which correspond to hydrogens attached to the anthracene α- and β-positions (C1 and C2, respectively). Correspondingly, signals at 127.2 and 132.6 ppm in the ^{13}C NMR spectrum correspond to α- and β-carbons (C1 and C2), while peaks at 126.6 and 118.4 ppm correspond to the quaternary carbons of the fused ring system (e.g., C4a) and the carbons linked to alkyne substituents (e.g., C9), respectively. The ^{1}H NMR spectrum of compound **4** is similar to that of **3**, but with the addition of a singlet at 7.27 ppm, corresponding to the spin-isolated and equivalent protons attached to C2 and C3 of the

(13) Bachmann, W. E. *Organic Synthesis*; Wiley: New York, 1955; Collect. Vol. III, p 841.

SCHEME 2

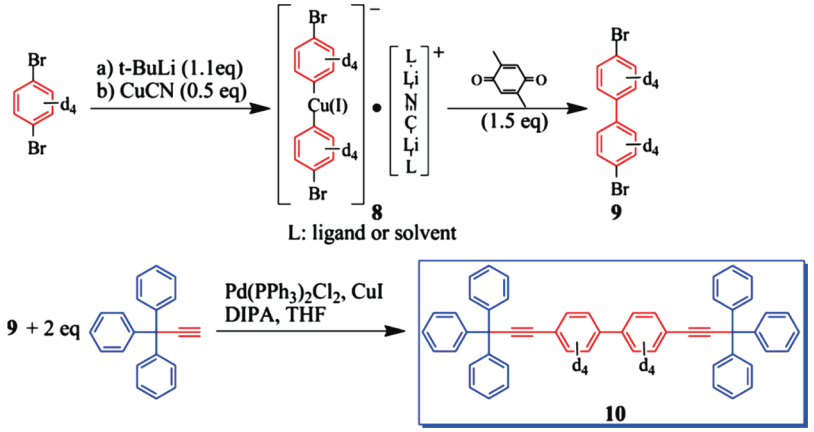

1,4-substituted naphthyl unit. The ^{13}C NMR spectrum is also very similar to that of **3**, except for the addition of a peak at 129.6 ppm, which also corresponds to the equivalent C2 and C3 of the naphthalene unit. Finally, the ^{1}H NMR spectrum of 4,4′-disusbtituted 1,1′-binaphthyl **5** consists of two doublets at 7.89 and 7.45 ppm (J = 7.3 Hz) from hydrogen atoms linked to C2 and C3 of each naphthyl unit, two doublets at 8.45 and 7.40 ppm (J = 8.3 Hz) due to hydrogen atoms linked to C5 and C8, and two doublets of doublets at 7.52 and 7.32 ppm (J = 8.3, 8.3 Hz), respectively, from hydrogen atoms linked to C6 and C7.

An isotopolog of compound **2** with a deuterated biphenylene rotator and protonated stators (**10**) was synthesized to determine its rotational dynamics using variable-temperature quadrupolar echo ^{2}H NMR in order to compare it with the VT CPMAS data. The deuterated biphenyl rotator **9** was constructed by electron transfer oxidation of the corresponding cuprate **8**.[14] The resulting 4,4′-dibromobiphenyl-d_8 was then coupled to 2 equiv of 3,3,3-triphenylpropyne using the same Sonogashira conditions as before (Scheme 2) to give **10**. The ^{13}C NMR spectrum of **10** is the same as that of **2** except that now the carbon atoms of the rotator are split into triplets while the stator carbon atoms give only singlets.

Thermal Analyses. Differential scanning calorimetry (DSC) analysis of **2**−**5** showed that all four compounds decompose prior to melting. This is shown by a sharp endotherm in the heating curve followed by a color change from white or pale yellow to dark brown. There was no crystallization on cooling. The heating curve remains smooth throughout the measurement until the decomposition, meaning that there are no phase changes (melting or solid-to-solid) and no residual solvent is expelled.

X-ray Crystal Structure Analysis of *o*-Xylene Clathrate 2. X-ray quality crystals of the *o*-xylene clathrate of rotor **2** were obtained by cooling an *o*-xylene solution from its boiling point down to 25 °C. X-ray diffraction data were collected at 100 K, and the structure was solved in the space group $P2_1/c$. The structure of **2** with the disordered *o*-xylene molecules is shown in Figure 2. As is often seen in rotor molecules, the two triphenylmethyl groups adopt a conformation where the trityl groups at the two ends of the structure adopt an *anti* conformation. The molecules have

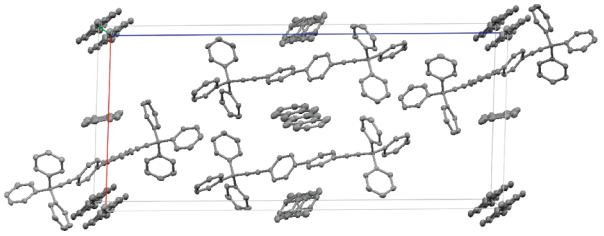

FIGURE 2. Unit cell of the *o*-xylene clathrate of **2** (hydrogens omitted for clarity) viewed down the *b*-axis.

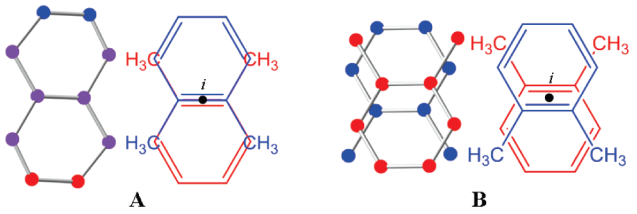

FIGURE 3. *o*-Xylene molecules disorder in two different forms as a result of inversion through a point (a) midway between the C_1 and C_2 atoms or (b) 0.4 Å inside the aromatic ring.

no center of symmetry, meaning that each carbon atom occupies a unique crystallographic site. The alkyne axle deviates slightly from linearity with the ipso carbon of the rotator, the center of the alkyne bond and the methane carbon of the stator forming an angle of 175° instead of 180°. The two phenyl groups in the biphenyl rotator are not coplanar but display a twist of 31.4°.

The two crystallographically distinct *o*-xylene molecules are highly disordered (Figure 3). On average, one appears as a naphthalene-shaped molecule as a result of the two possible orientations of the *o*-xylene molecules, which occupy sites related by an inversion center at the center of the C_1−C_2 bond (Figure 3a), each with occupancy factors of 0.5. The other *o*-xylene molecule is also disordered, but the sites occupied by C_1 and C_2 are not shared by both disordered molecules. Instead, they overlap each other such that the two C_1−C_2 bonds are parallel but separated by 0.8 Å. The net result is that the two possible orientations of the molecule occupy sites related by an inversion center located 0.4 Å inside the aromatic ring (Figure 3b). Again, the occupancy factor for each site is 0.5.

(14) Miyake, Y.; Wu, M.; Rahman, M. J.; Kuwatani, Y.; Iyoda, M. *J. Org. Chem.* **2006**, *71*, 6110–6117.

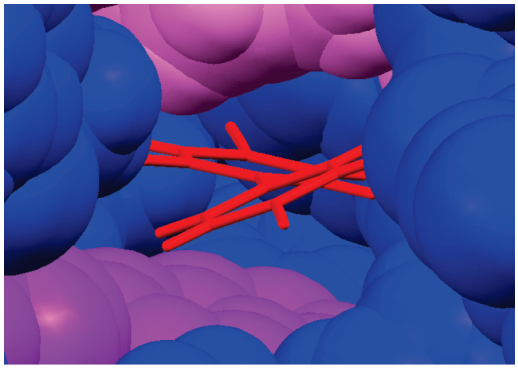

FIGURE 4. Close up of the rotator in the crystal, shown in red capped sticks, with neighboring solvent (purple) and rotor (blue) molecules illustrated in space-filling model.

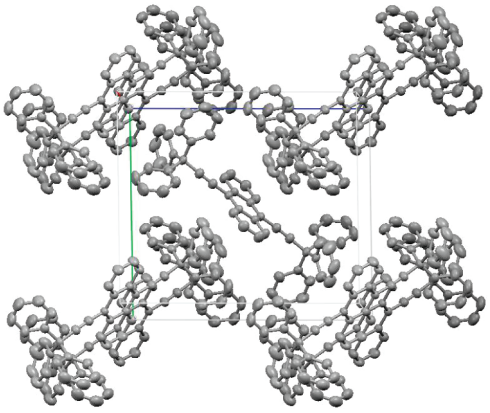

FIGURE 5. Unit cell of **3** (hydrogens omitted for clarity) viewed down the *a*-axis.

The two rings of the biphenyl rotator each participate in staggered π-stacking interactions with the two types of disordered *o*-xylene, which occupy alternating channels through the crystal. Closer examination of the biphenyl rotator, shown in red capped sticks, in a space-filling environment in Figure 4 shows the aforementioned staggered π-stacking interactions of the rotator phenylenes with the solvent molecules (purple). The figure also shows the shape of the cavity made by the surrounding solvent molecules (purple) and neighboring rotor molecules (blue) occupied by the rotator.

X-ray Crystal Structure Analysis of 3. Solvent-free X-ray quality crystals of **3** were grown by slowly evaporating a 90:5:5 hexanes/toluene/dichloromethane solution at room temperature. The structure was solved at 298 K in the monoclinic space group $P2_1/n$ with 1/2 molecule per asymmetric unit and 2 molecules per unit cell. The unit cell is shown in Figure 5. The alkyne axles in this case also deviate from linearity but to a larger degree with the ipso carbon of the rotator, center of the alkyne bond, and methane carbon of the stator forming an angle of 171°. The triphenylmethyl groups again adopt a staggered conformation. In this case, however, the rotor molecules possess a center of inversion, so that each carbon atom in the structure is crystallographically equivalent to another related by the inversion symmetry operation. The molecules pack such that the triphenylmethyl stators surround the anthryl rotators of neighboring

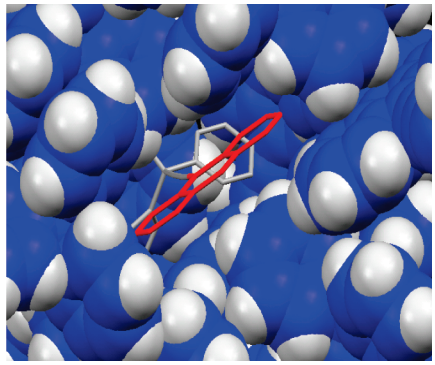

FIGURE 6. Close up of anthryl rotator (red) in the "pocket" created by stators of neighboring molecules.

TABLE 1. Unit Cell Parameters for *o*-Xylene Clathrate of 2 and Solvent-Free 3

	2	3
formula	$C_{54}H_8D_{30}$, C_8H_{10}	$C_{56}H_8D_{30}$
formula weight	822.68	740.48
crystal system	monoclinic	monoclinic
space group	*P*21/*c*	*P*21/*n*
a (Å)	15.9910(13)	8.5969(12)
b (Å)	7.5955(6)	14.440(2)
c (Å)	36.383(3)	16.362(2)
α (deg)	90.00	90.00
β (deg)	91.0640(10)	102.739(3)
γ (deg)	90.00	90.00
V (Å^3)	4418.3(6)	1981.1(5)
Z	4	2
T (K)	100	298

molecules so that the "pocket" fits the rotator tightly (Figure 6). Unit cell parameters for **2** and **3** are given in Table 1.

Solid-State CPMAS ^{13}C NMR. The CPMAS ^{13}C NMR spectra of compound **1** reported in ref 12 was acquired with a cross-polarization time of 50 μs, and the resulting spectrum varied from the slow to the fast exchange regime as the temperature varied from 214 to 308 K. The low temperature spectrum consisted of two well-resolved signals at 128.5 and 132 ppm that were assigned to sites related by a 180° rotation, which were shown to coalesce at 280 K and to sharpen at higher temperatures. The CPMAS ^{13}C NMR spectra of compounds **2**−**5** were systematically explored with cross-polarization times of 50, 500, 5,000, and 15,000 μs in order to determine the optimal conditions to highlight the protonated and nonprotonated carbons of the rotator, as well as the contact times required to transfer polarization to the carbon atoms of the dialkyne axle and the deuterated stator, which are significantly more distant from the H-donors in the center of the molecules. Representative CPMAS ^{13}C NMR spectra of compound **2** obtained at 298 K with contact times of 50, 500, and 15,000 μs are shown in Figure 7 along with the corresponding solution spectrum ($CDCl_3$). Full spectra obtained with similar contact times for compounds **2**−**5** are included in Supporting Information (Figure S20).

As illustrated in Figure 7, the four signals of the biphenyl rotator in the spectrum of **2** in $CDCl_3$ occur at 140.0 (C_1), 132.1 (C_2), 127.2 (C_3), and 122.9 ppm (C_4) (Figure 7d). As it is apparent from the spectrum in Figure 7a, a contact time of

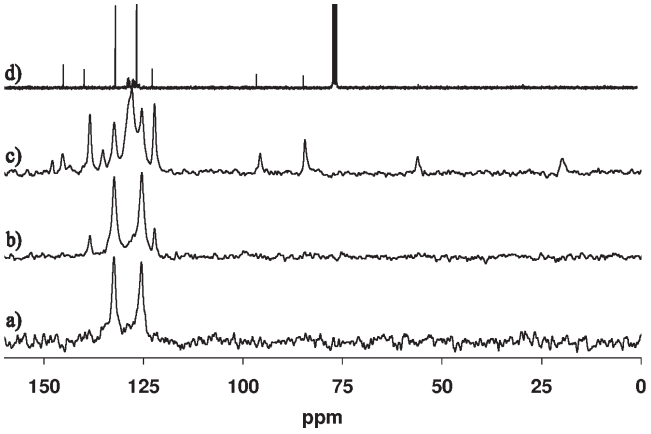

FIGURE 7. CPMAS ^{13}C NMR spectra of the *o*-xylene clathrate of compound **2** acquired with contact times of (a) 50 μs, (b) 500 μs, and (c) 15,000 μs with the solution spectrum (d) added for comparison.

50 μs reveals only two relatively sharp signals, which are assigned to protonated carbons C_2 and C_3. The spectrum in Figure 7b illustrates the effect of increasing the contact time to 500 μs with the two types of ipso carbons in the biphenyl moiety (C_1 and C_4) starting to become visible at 138.5 and 122.2 ppm. A further extension of the contact time to 15 ms reveals all the signals in the structure, including those of the *o*-xylene-d_{10} solvent with methyl groups at 19.8 ppm and aromatic carbons overlapping with those of compound **2**. It is worth noting that there are more signals in the full CPMAS spectrum than in the one solution, as expected from the lower molecular symmetry in the solid state. This is particularly evident with the signals corresponding to the ipso carbons of the trityl stator. While only one signal is observed in solution at 145.2 ppm, three signals corresponding to six crystallographically nonequivalent *ipso* carbons are observed in the solid state at 143.4, 145.2, and 147.7 ppm. However, relatively narrow and unique signals for each of the quaternary trityl (56.1 ppm), alkyne (95.7 and 84.4 ppm), and biphenyl carbons (138.5, 132.4, 125.4, and 122.2 ppm) indicate that the two halves of the molecule are coincidentally isochronous despite being crystallographically nonequivalent. Single resonances for the protonated carbons of the biphenyl group are consistent with two scenarios: (a) a static structure with insufficient chemical shift dispersion to resolve the two sites related by 180° rotation or (b) a rotational motion takes place in the fast exchange regime at ambient temperature (see below).

In order to determine how the signal intensities are affected by varying contact times, the intensities of several signals from the spectra in Figure 7 were plotted with respect to the cross-polarization, or contact time, in Figure 8. From this experiment one can see that the ^{13}C signal enhancement is strongly dependent on the proximity of each carbon to the ^{1}H nuclei. The aromatic ^{13}C attached to the ^{1}H nuclei reach their maximum intensities within 500 μs, whereas the nonprotonated ^{13}C nuclei of the biphenyl rotator located 2 bonds away from the ^{1}H nuclei reach their maximum intensity around 5,000 μs. The ^{13}C nuclei located even farther away do not reach their maximum even after 15,000 μs. It is also clear from the plot that the rotator signals reach their maxima and begin to decay with rates determined by the spin−lattice relaxation in the rotating frame, $T_{1\rho}$, which

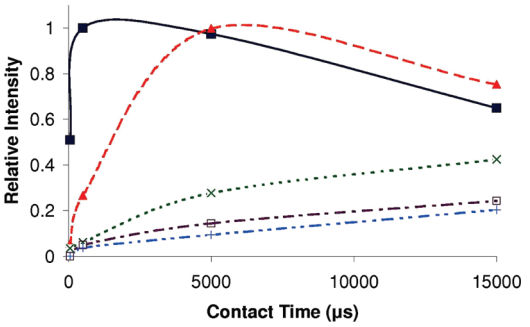

FIGURE 8. Relative intensities of protonated rotator carbon (■), nonprotonated rotator carbon (▲), alkyne carbon (×), quaternary carbon (□), and trityl ipso carbon (+) signals of **2** with respect to contact time.

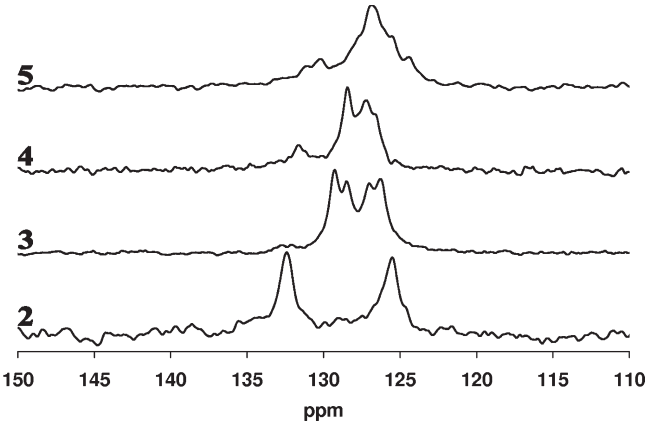

FIGURE 9. Isolated CPMAS ^{13}C rotator signals of compounds **2**−**5** at short contact time (50 μs).

depends on molecular motions with frequencies on the order of the spin locking fields (ca. 10−20 kHz), which are close to rotary motions observed in other molecular gyroscopes.[2a−d,7,8]

The NMR signals of the protonated rotators of all compounds can be isolated in the same manner as illustrated in Figure 9 such that the only ^{13}C signals visible at short contact times correspond to the protonated carbons. The CPMAS ^{13}C NMR spectra of compounds **3**−**5** at intermediate and long contact times are available in Supporting Information (Figure S20).

Variable-Temperature CPMAS ^{13}C NMR Measurements of the *o*-Xylene Clathrate of 2. As shown in Figure 10, the 311 K spectrum of **2** acquired with a 50 μs contact time consists of two relatively sharp signals corresponding to C2/C2′ and C3/C3′, respectively. A modest broadening of the C2/C2′ signal at ca. 132 ppm was observed when the temperature was lowered to 199 K (Figure 10). While one could interpret signal broadening in terms of a very rapid two-site exchange that barely begins to enter the intermediate exchange regime, one should also consider a situation where the two sites are actually static but have temperature-dependent chemical shifts that change the extent of overlap.

We reasoned that changes in rotational dynamics induced with the help of simple structural perturbations could help determine whether the changes in line shape in Figure 10 could be assigned to fast motion of the biphenylene group. As a simple test we decided to prepare and analyze

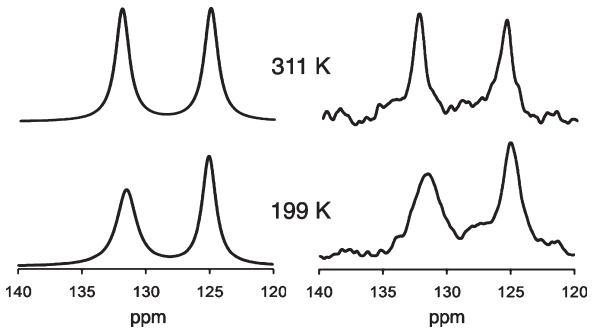

FIGURE 10. Experimental (right) and simulated (left) solid-state CPMAS ^{13}C NMR of the protonated aromatic signals of **2**. The frequencies of the two sites were assumed to be the same as those in the solvent-free sample shown in Figure 11 at 196 K, and the rate constants for rotational exchange used for fitting are based on the results of the VT ^{2}H NMR experiments shown in Figure 12. The exchange rates in the simulations are 1.0×10^{3} s^{-1} at 199 K and 9.0×10^{5} s^{-1} at 311 K.

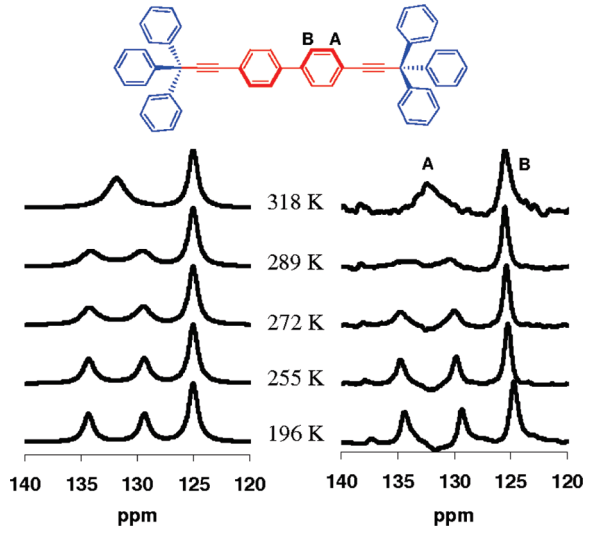

FIGURE 11. Experimental (right) and simulated (left) solid-state CPMAS ^{13}C NMR of **2**. The rotational rate constants used for fitting, from bottom to top, are (s^{-1}) 1.2, 50, 173, 253, and 2990.

a solvent-free sample with a solid obtained by rapid evaporation from CH_2Cl_2. We were able to confirm the lack of solvent in a solid material that appeared amorphous. However, analysis by X-ray powder diffraction revealed broad signals with a pattern completely different from that of the *o*-xylene clathrate, suggesting the formation of a crystalline solid (Figure S23 in Supporting Information). As it was hoped for, analysis of this sample by VT-CPMAS ^{13}C NMR displayed line shape changes characteristic of a dynamic process in the intermediate exchange regime (Figure 11). Comparison of the spectra acquired at 318 and 196 K showed that the signal at 132.4 ppm in the high-temperature spectrum splits into two signals at 134.4 and 129.3 ppm as the temperature is lowered. In going from lower to higher temperature, the spectra showed coalescence of the signals at 134.4 and 129.3 ppm as the temperature increased between 289 and 318 K. The merging peaks correspond to the carbons that are *ortho* to the alkyne linkages, carbon A in Figure 11, and their coalescence occurs as the biphenyl jumps between the two crystallographically different sites related by the 180° rotation. While the signal corresponding to carbon B at 124.9 ppm must undergo the same site-exchange process, the lack of splitting at low temperatures indicates that the two sites must have the same chemical shift.[15] Approximate exchange rates obtained by simulation of the line shapes varied from 1 s^{-1} at 196 K to 2,990 s^{-1} at 318 K. An Arrhenius plot constructed with the frequency and temperature data revealed an activation energy of 8.7 kcal/mol and a pre-exponential factor of 4.9×10^{9} s^{-1}.

Having confirmed a dynamic processes in the kilohertz regime in solvent-free samples of **2** and with hints that rotation in the *o*-xylene structure may be even faster, we decided to investigate the dynamics of the latter by variable-temperature wide-line quadrupolar echo ^{2}H NMR. To carry out those measurements, we prepared compound **10** with a natural abundance stator and a deuterated rotator (Scheme 2).

Variable-Temperature ^{2}H Quadrupolar Echo Measurements with the *o*-Xylene Clathrate of 10. It is known that variable-temperature ^{2}H NMR with static powder samples is a powerful method to determine internal molecular dynamics of solids in a range that covers ca. $10^{3}-10^{7}$ s^{-1}.[16] Deuterium NMR is largely dominated by the orientation-dependent interaction between the nuclear spin and electric quadrupole moment at the nucleus that gives rise to a broad spectrum known as a Pake or powder pattern. Changes in the spectra occur when the C$-^{2}H$ bonds experience reorientations that reduce their magnetic interactions by dynamic averaging.[17] Robust methods have been implemented to study the rotation of phenylene groups, which are known to have quadrupolar coupling constants (QCC) of ca. 180 kHz.[18] Crystalline samples with no phase transitions display spectra that change as a function of temperature in a predictable manner, such that for structurally well-characterized dynamic processes the experimental spectrum can be simulated with a model that considers the trajectories of motion and a suitable exchange rate.

^{2}H NMR experiments were carried out with a standard quadrupolar echo sequence on samples of compound **10** freshly crystallized from *o*-xylene. As shown in Figure 12, measurements were carried out over a similar temperature range as the CPMAS ^{13}C NMR experiments in Figures 10 and 11. As the ^{2}H label represents only 0.97% of the total mass in the sample, at least ca. 2048 transients with 20 s between pulses had to be averaged to obtain reasonable spectra. The spectrum acquired at 188 K approaches the slow exchange regime, and the simulation suggests a 180° rotation with an exchange rate of 7.0×10^{3} s^{-1}. At the other extreme of the temperatures analyzed, the spectrum is also consistent with a fast flipping motion, but the line shape is slightly narrower than that expected from a simple 180°

(15) While differences in cross polarization efficiencies and relaxation properties make uncalibrated integration of CPMAS ^{13}C NMR spectra quantitatively unreliable, the integration of signals A and B remained relatively constant as a function of temperature, in agreement with the expected assignments.

(16) Hoatson, G. L.; Vold, R. L. *NMR* **1994**, *32*, 1–67.
(17) (a) Kamihira, M.; Naito, A.; Tuzi, S.; Saito, H. *J. Phys. Chem. A* **1999**, *103*, 3356–3363. (b) Hiraoki, T.; Kogame, A.; Norio, N.; Akihiro, T. *J. Mol. Struct.* **1998**, *441*, 243–250. (c) Zhang, H.; Bryant, R. G. *Biophys. J.* **1997**, *72*, 372. (d) Naito, A.; Izuka, T.; Tuzi, S.; Price, W. S.; Hayamizu, K.; Saito, H. *J. Mol. Struct.* **1995**, *355*, 55–60.
(18) Mantsch, H. H.; Saito, H; Smith, I. C. P. *Prog. NMR Spectrosc.* **1977**, *11*, 211–272.

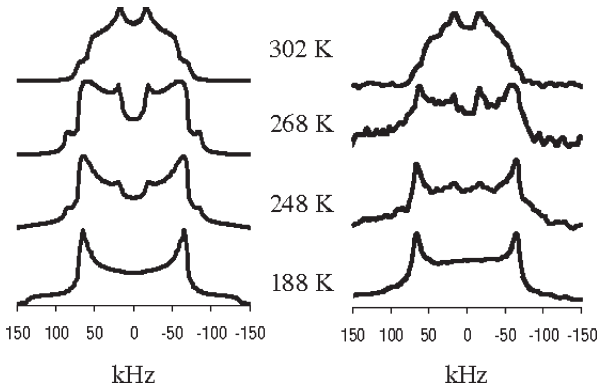

FIGURE 12. Experimental (right) and simulated (left) solid-state ^{2}H quadrupolar echo NMR of **10**. The rotation rate constants used for fitting, from bottom to top, are (s^{-1}) 7.0×10^3, 7.0×10^5, 1.7×10^6, and 1.5×10^7.

rotation. The model used in the ^{2}H NMR simulation involves the expected 2-fold flipping motion with an additional ±15° libration in the fast exchange limit, as expected for a rotator with relatively large amplitude oscillation at the bottom of its energy well.[19] Intermediate spectra were also simulated with the 180° rotational model with the exchange frequencies listed in the figure. An Arrhenius plot built with the temperature and frequency data gave an energy barrier of 7.4 kcal/mol and a pre-exponential factor of 2.5×10^{12} s^{-1}. With two transition states related by 180° per cycle, our results indicate that the intrinsic gas potential of biphenyl with four transition states of ca. 1.4 and 1.6 kcal/mol for coplanar and orthogonal orientations of the two rings, respectively,[20] does not play a significant role in the solid state.

^{2}H NMR experiments carried out with the solvent-free sample (Supporting Information, Figure S24) provided spectra in the slow exchange regime, as expected from its lower pre-exponential factor. It should be noted that the ^{2}H NMR results in Figure 12 do not have sufficient kinetic resolution to determine whether the two crystallographically nonequivalent phenyl groups have distinguishable dynamics. While the error in the ^{2}H NMR data has been estimated as high as 2 kcal/mol, it is also notable that the activation energy for ^{2}H NMR rotational exchange of the biphenylene group in *o*-xylene-containing crystals of **10** is ca. 4−5 kcal/mol lower than that reported for the rotation of a single phenylene in benzene-containing crystals of **1** in the same temperature range (E_a = 11.3−12.8 kcal/mol).[7a,b,12] Considering that differences in the amount of free volume may be a possible explanation for this difference, we analyzed the packing coefficient of crystals **1** and **2** using the increment approach proposed by Gavezzotti.[21] Packing coefficients were defined by Kitaigorodski as the volume of the molecules in the unit cell relative to the total volume of the unit cell.[22] Values calculated for compounds **1** and **2** of 0.729 and 0.730, respectively, suggest that the average free volume cannot account for the different barriers. While computational studies and additional experiments will be needed, it is possible that local motion and correlated effects of the adjacent phenylenes of **2** may be responsible for their lower barrier.

A comparison of the activation parameters obtained for the solvent-free solid by VT CPMAS ^{13}C NMR with those of the crystalline clathrate by VT quadrupolar echo ^{2}H NMR is very interesting. While the activation energies of 8.7 and 7.4 kcal/mol for the solvent-free and solvated solids, respectively, are within the range of experimental uncertainties, the magnitudes of their pre-exponential factors, *A*, are quite different. Also known as the "frequency factor" or "attempt frequency,"[23] the pre-exponential factor represents the highest rotational frequency that would be possible in a hypothetical structure with no energy barrier. Its value depends on the moment of inertia of the rotator, the torsional mode that describes the oscillation of the central phenylene, and the vibrational dynamics of the crystal. A pre-exponential factor of 2.5×10^{12} s^{-1} for the crystalline clathrate is consistent with the values obtained previously for phenylene rotators in other crystalline environments[2,4,7,8] and is close to the value calculated for a free rotator on the basis of its moment of inertia.[24] However, a pre-exponential factor of only 4.9×10^9 s^{-1} for the desolvated sample is 3 orders of magnitude lower! Given that it is the same molecular structure, it seems likely that differences in rotational motion arise from differences in their solid-state environments. While conformational and packing differences are likely, differences resulting in steric hindrance should affect primarily the activation the energy. An important difference between the solvent containing and desolvated crystals that may contribute to their different pre-exponential factors is the extent of their long-range order, which is expected to affect their lattice dynamics.[25]

We had noticed that peaks in the CPMAS spectra of the solvent-free solid are significantly broader than those of the crystalline clathrate, suggesting a disordered environment. To confirm that there are large differences in long-range order between the two samples, we analyzed their X-ray powder patterns acquired at a wavelength of 1.542 Å (Cu Kα).[26] The line-widths of the solvent-free powder samples at half the maximum intensity (e.g., fwhm ≈ 0.27° at 2Θ = 16.8°, Figure S23) are ca. 2.7 times as large as those of samples from freshly powdered crystals with *o*-xylene (e.g., fwhm ≈ 0.1° at 2Θ = 17.6°). From the Scherrer equation,[26] one can estimate that broadening in the solvent-free sample corresponds to a domain size of ca. 33 nm. Thus, while the pre-exponential factors of highly crystalline rotor molecules with phenylene rotators have values in the terahertz regime (ca. 10^{12} s^{-1}), we speculate that changes in lattice vibrations as a function of disorder may result in less efficient mechanisms for rotational motion.

Conclusions. We have shown that the rotator signals of compounds **2**−**5**, as previously shown for **1**, are all visible and with no interference from the carbons of their trityl stators at contact times of ca. 50 μs. While the strategy is ideal

(19) (a) Aliev, A. E.; Harris, K. D. M.; Champkin, P. H. *J. Phys. Chem. B* **2005**, *109*, 23342–23350. (b) Hallock, K. J.; Lee, D. K.; Ramamoorthy, A. *J. Chem. Phys.* **2000**, *113*, 11187–11193.

(20) (a) Johansson, M. P.; Olsen, J. *J. Chem. Theor. Comp.* **2008**, *4*, 1460. (b) Bastiansen, O.; Samdal, S. *J. Mol. Struct.* **1985**, *128*, 155.

(21) Gavezzotti, A. *J. Am. Chem. Soc.* **1990**, *105*, 5220–5225.

(22) Kitaigorodskii, A. I. *Molecular Crystals and Molecules*; Academic Press: New York, 1973.

(23) Laidler, K. J. *Chemical Kinetics*, 3rd ed.; Benjamin-Cummings, 1997

(24) Kawski, A. *Crit. Rev. Anal. Chem.* **1993**, *23*, 459–529.

(25) Burns, G. *Solid State Physics*; Academic Press: San Diego, CA, 1985.

(26) West, A. R. *Solid State Chemistry and Its Applications*; John Wiley & Sons: New York, 1984.

for the study of dynamic processes in the solid state, the method suffers the inherent limitations of the VT CPMAS ^{13}C NMR experiment and will be useful when the exchanging signals have sufficiently different resonance frequencies with structurally well-determined dynamic processes that are thermally accessible in the range of ca. 100 Hz to 10 kHz.[2c] The rotational dynamics of crystalline samples of the molecular rotor with a biphenylene rotator obtained with a combination of VT CPMAS ^{13}C NMR (compound **2**) and static ^{2}H NMR (compound **10**) revealed remarkably similar activation energies and pre-exponential factors that correlate with the extent of order. Given that many previous reports with ordered crystalline substrates are in agreement with ordered crystals of **2** and give pre-exponential values in the 10^{12} s^{-1} range, it was speculated that the 3 orders of magnitude lower value measured in the lower quality crystals may be due to the changes in lattice vibrations, which may be needed to couple with rotator torsional modes to provide a good mechanism for internal rotations. Further experiments with other crystal and glass forming structures accompanied by computational studies will be carried out to investigate this possibility.

Experimental Section

IR spectra were obtained with a ATR-FTIR instrument. ^{1}H and ^{13}C spectra were acquired on a spectrometer at frequencies of 500 and 125 MHz, respectively, with $CDCl_3$ as the solvent. Solid-state CPMAS ^{13}C NMR spectra were obtained at 75 MHz. DSC analyses were recorded between room temperature and the melting/decomposition temperature as determined by a standard melting point apparatus. Mass spectra were acquired on an FT-ICR-MS with the MALDI ion source.

3,3,3-Tri-d_5-phenylpropyne (7). A 100-mL three-neck round-bottomed flask equipped with a reflux condenser was charged with d_6-benzene (10.0 g, 0.119 mmol), carbon tetrachloride (2.0 mL, 0.022 mmol), and 20 mL of 1,1,2,2-tetrachloroethane. The solution was sparged with argon for 30 min and then cooled to 0 °C. Aluminum chloride (3.1 g, 0.023 mmol) was then added slowly with stirring. The solution was stirred for 15 min before being allowed to warm to room temperature. The solution was heated for 90 min and then cooled. Solution was quenched with 1 M HCl, and the organics were extracted with methylene chloride and dried over magnesium sulfate. The crude product was purified by column chromatography (hexanes/ethyl acetate = 9:1) to afford 3.24 g of **7** (50.1% isolated yield).[11] The trityl chloride was then dissolved in 10 mL of acetyl chloride and heated to reflux for 1 h. Acetyl chloride solvent was then removed *in vacuo*, and 100 mL of dry benzene was added and subsequently removed *in vacuo*. An additional 500 mL of dry benzene was then added followed by 100 mL of ethynylmagnesium bromide (0.5 M in THF) via cannula. The solution was heated to reflux overnight. The cooled solution was then quenched with a saturated ammonium chloride solution, and the organics were extracted with methylene chloride and dried over magnesium sulfate. The crude product was purified by column chromatography (hexanes) to afford 1.80 g of **6** (69.8% isolated yield) as a white solid.

1,4-Bis(3,3,3-tri-d_5-phenylpropynyl)benzene (1). The synthesis and characterization of compound **1** has been described in the literature.[11]

4,4′-Bis(3,3,3b-tri-d_5-phenylpropynyl)biphenyl (2). A 100-mL three-neck round-bottomed flask equipped with a reflux condenser was charged with 40 mL of THF, 20 mL of diisopropyl amine, and a magnetic stir bar. The 3,3,3-tri-d_5-phenyl-1-propyne (0.209 g, 0.738 mmol) and 4,4′-dibromobiphenyl (0.138 g, 0.443 mmol) were dissolved in the solution, which was then sparged with argon for 1 h. Bis(triphenylphosphine) palladium(II) chloride (0.037 g, 0.052 mmol) and copper(I) iodide (0.012 g, 0.064 mmol) were added, and the reaction was heated to reflux for 24 h under argon. Reaction progress was monitored by thin layer chromatography. Upon completion, the reaction mixture was washed with saturated ammonium chloride solution, and the organics were extracted with methylene chloride and dried over magnesium sulfate. The crude product was purified by column chromatography (hexanes/C_6H_6/CH_2Cl_2 = 90:5:5) to afford 0.125 g (47.4% isolated yield) of **2** as a white solid, mp dec > 253 °C. ^{1}H NMR (500 MHz, $CDCl_3$): δ 7.56 (dd, 4H, J = 2.0, 8.5 Hz), 7.53 (dd, 4H, J = 2.0, 8.5 Hz). ^{13}C NMR (125 MHz, $CDCl_3$) δ 145.1, 139.9, 132.1, 128.7 (t, $^{1}J_{CD}$ = 24.0 Hz), 127.5 (t, $^{1}J_{CD}$ = 23.4 Hz), 126.8, 126.3 (t, $^{1}J_{CD}$ = 21.7 Hz), 122.8, 96.6, 84.8, 56.0. FTIR (solid HATR, cm^{-1}): 3079, 3062, 3032, 2274, 1559, 1492, 1362, 1327, 824. HRMS (MALDI-ICR) $C_{54}H_8D_{30}$: calcd 716.4826; found 716.4879.

9,10-Bis(3,3,3-tri-d_5-phenylpropynyl)anthracene (3). Compound **3** was prepared using the same procedure as for compound **1** in 55.9% yield (0.156 g) as a bright yellow solid, mp dec > 312 °C. ^{1}H NMR (500 MHz, $CDCl_3$): δ 8.56 (m, 4H, $J_{ax} = J_{a'x'}$ = 9.0 Hz, $J_{xx'}$ = 8.0 Hz, $J_{aa'}$ = 0.8 Hz, $J_{ax'} = J_{a'x}$ = 2.1 Hz), 7.51 (m, 4H, $J_{ax} = J_{a'x'}$ = 9.0 Hz, $J_{xx'}$ = 8.0 Hz, $J_{aa'}$ = 0.8 Hz, $J_{ax'} = J_{a'x}$ = 2.1 Hz), 7.38 (s, residual trityl protons), 7.33 (s, residual trityl protons). ^{13}C NMR (125 MHz, $CDCl_3$): δ 145.1, 132.6, 128.9 (t, $^{1}J_{CD}$ = 23.9 Hz), 127.7 (t, $^{1}J_{CD}$ = 23.9 Hz), 126.6, 126.3 (t, $^{1}J_{CD}$ = 21.7 Hz), 118.4, 108.4, 82.5, 57.0. FTIR (solid HATR, cm^{-1}): 3059, 2274, 1559, 1435, 1392, 1362, 1326, 826, 770. HRMS (MALDI-ICR) $C_{56}H_8D_{30}$: calcd 740.4826; found 740.4889.

1,4-Bis(3,3,3-tri-d_5-phenylpropynyl)naphthalene (4). Compound **4** was prepared using the same procedure as for compound **1** in 67.7% yield (0.1832 g) as a white solid, mp dec > 247 °C. ^{1}H NMR (500 MHz, $CDCl_3$): δ 8.36 (m, 2H, $J_{ax} = J_{a'x'}$ = 8.9 Hz, $J_{xx'}$ = 8.1 Hz, $J_{aa'}$ = 0.8 Hz, $J_{ax'} = J_{a'x}$ = 2.1 Hz), 7.69 (s, 2H), 7.54 (m, 2H, (m, 2H, $J_{ax} = J_{a'x'}$ = 8.9 Hz, $J_{xx'}$ = 8.1 Hz, $J_{aa'}$ = 0.8 Hz, $J_{ax'} = J_{a'x}$ = 2.1 Hz), 7.46 (s, residual trityl protons), 7.38 (s, residual trityl protons), 7.33 (s, residual trityl protons). ^{13}C NMR (125 MHz, $CDCl_3$): δ 145.1, 133.5, 129.6, 128.8 (t, $^{1}J_{CD}$ = 23.9 Hz), 127.6 (t, $^{1}J_{CD}$ = 24.0 Hz), 127.1, 126.6, 126.4 (t, $^{1}J_{CD}$ = 23.5 Hz), 102.0, 83.4, 56.4. FTIR (solid HATR, cm^{-1}): 3059, 3047, 2277, 1560, 1384, 1362, 1327, 846, 826, 768. HRMS (MALDI-ICR) $C_{52}H_6D_{30}$: calcd 690.4760; found 690.4704.

(±)-4,4′-Bis(3,3,3-tri-d_5-phenylpropynyl)-1,1′-binaphthyl (5). Compound **5** was prepared using the same procedure as for compound 1 from racemic starting material in 92.3% yield (0.260 g) as a white solid, mp dec > 268 °C. ^{1}H NMR (500 MHz, $CDCl_3$): δ 8.46 (d, 2H, J = 8.4 Hz), 7.90 (d, 2H, J = 7.3 Hz), 7.53 (dd, 2H, J = 7.1, 7.1 Hz), 7.47 (d, 2H, J = 7.3 Hz), 7.46 (d, 2H, J = 8.4 Hz), 7.33 (dd, 2H, J = 7.3, 7.3 Hz). ^{13}C NMR (125 MHz, $CDCl_3$): δ 145.2, 138.6, 133.7, 132.6, 129.8 128.8 (t, $^{1}J_{CD}$ = 24.3 Hz), 127.6 (t, $^{1}J_{CD}$ = 24.0 Hz), 127.2, 126.8, 126.7, 126.6, 126.5, 121.3, 101.0, 83.6, 56.5. FTIR (solid HATR, cm^{-1}): 3089, 3052, 2274, 1575, 1381, 1362, 1326, 825, 758. LRMS (MALDI-TOF) $C_{62}H_{12}D_{30}$: calcd 816.52; found 816.52.

4,4′-Dibromo-d_8-biphenyl (9). A dry 500-mL round-bottom flask was charged with 1,4-dibromobenzene-d_4 (120 mg, 0.507 mmol), and 30 mL of dry tetrahydrofuran. The solution was cooled to −78°, *tert*-butyllithium (0.37 mL, 0.56 mmol) was added, and the solution was stirred for 90 min. Copper(I) cyanide (22 mg, 0.25 mmol) was then added, and the solution was stirred vigorously as it warmed up to room temperature. Upon reaching room temperature, 2,5-dimethyl-*p*-benzoquinone (104 mg, 0.761 mmol) was added, and the resultant dark blue solution was stirred at room temperature for 3 h. The reaction was then quenched with 20 mL of 2 M HCl, and the organics were extracted with diethyl ether and dried over $MgSO_4$. The crude product was purified by column chromatography

(100% hexanes, silica) to afford 121 mg of **9** (75% isolated yield) as a white solid, mp 162 °C. ^{1}H NMR (500 MHz, $CDCl_3$): δ. ^{13}C NMR (125 MHz, $CDCl_3$): δ 145.2, 138.6, 133.7, 132.6, 129.8 128.8 (t, $^1J_{CD}$ = 24.3 Hz), 127.6 (t, $^1J_{CD}$ = 24.0 Hz), 127.2, 126.8, 126.7, 126.6, 126.5, 121.3, 101.0, 83.6, 56.5. FTIR (solid HATR, cm^{-1}): 2274, 1569, 1375, 1362, 1326, 825, 758. LRMS (MALDI-TOF) $C_{12}D_8Br_2$: calcd 317.95; found 317.96.

4,4′-Bis(3,3,3-triphenylpropynyl)biphenyl-d_8 (10). Compound **10** was prepared using the same procedure as for compound **1** in 46% yield (47 mg) as a white solid, mp dec > 253 °C. ^{1}H NMR (300 MHz, $CDCl_3$): δ 7.29−7.45 (m, 30H), ^{13}C NMR (75 MHz, $CDCl_3$): δ 145.2, 139.7, 131.6 (t, $^1J_{CD}$ = 25.0 Hz), 129.1, 128.0, 127.0, (t, $^1J_{CD}$ = 24.0 Hz), 126.5 (t, $^1J_{CD}$ = 25.0 Hz), 122.6, 96.6, 84.8, 56.1. FTIR (solid HATR, cm^{-1}): 3082, 3058, 3031, 2278, 2251, 1596, 1490, 1446, 1398, 1327, 1033, 755. LRMS (MALDI-TOF) $C_{54}H_{30}D_8$: calcd 695.35; found 695.33.

Acknowledgment. The National Science Foundation supported this work through grant DMR-0605688.

Supporting Information Available: Synthetic procedures, spectroscopic data for all compounds, and crystallographic information files in CIF format for compounds **2** and **3**. This material is available free of charge via the Internet at http://pubs.acs.org.